

Analysis of interfacial stresses distribution in steel beams strengthened with thin composite plates and subjected to the thermo-mechanical loading

Ismail Bensaid*¹, Bachir Kerboua² and Mohamed Azzeddine Kadache¹

¹IS2M Laboratory, Faculty of Technology, Mechanical engineering Department,
University of Abou Beckr Belkaid (UABT), Tlemcen, Algeria

²Faculty of Technology, Mechanical engineering Department, University of Abou Beckr Belkaid (UABT),
Tlemcen, Algeria

(Received March 23, 2019, Revised March 22, 2020, Accepted April 24, 2020)

Abstract. Nowadays, the use of carbon fiber reinforced plastics (CFRP) plates for strengthening and repairing of structures degraded by their environment have attracted growing interest and are considered to be the most promising materials for applications in structural engineering. One of the main features of the reinforced beam is the significant stress concentration in the adhesive at the ends of CFRP plate; consequently, debonding failure may occur at the plate ends due to a combination of high shear and normal interfacial stresses. These stresses between a beam and a soffit plate, within the linear elastic range, have been addressed by numerous analytical investigations. This paper provides an analytical model for prediction of interfacial stresses in a reinforced steel beam under mechanical as well as thermal loads. The combined effects of the interface slip and both adherend shear deformations on the structural behavior are also incorporated in the current investigation. The present new model needs only one differential equation to determine both shear and normal interfacial stress whereas the others solutions need two differential equations. To verify the validity of the present model, the results are compared with those available in the literature. The effects of the physical and geometric parameters of the CFRP plate and adhesive layer on the maximum values of the interfacial stresses distributions are investigated.

Keywords: bi-material interface; adhesive bonding; thermal effects; interface slip; externally bonded plates; interfacial stresses; adherend deformation; strengthening

1. Introduction

For the past few decades externally bonded fiber reinforced polymer (FRP) composites are used for strengthening existing reinforced concrete and steel structures (Kerboua *et al.* 2013, Draiche *et al.* 2014, Chikh *et al.* 2017, Merdaci *et al.* 2016). This technique has numerous advantages such as increasing the strength and stiffness of an existing beam with minimal interference to the surrounding environment. The use of externally bonded thin FRP soffit plates has become very popular in recent years due to the favourable mechanical and durability properties of FRP composites. Under external loading, tensile force is generated within the bonded plate which is in

*Corresponding author, Ph.D., E-mail: bensaidismail@yahoo.fr

turn transferred to the original beam through the adhesive layer. This process generates interfacial shear and normal stresses in the adhesive layer. The concentration of interfacial stresses is the highest at the plate ends due to the geometric discontinuity at this location. The combination of high interfacial shear and normal stresses at the plate end commonly leads to a debonding failure of the plate from the original beam in a brittle manner well before the full flexural strength of the plated beam is attained. Several closed-form solutions have been developed over the last two decades to quantify the interfacial stresses near the ends of the plate; see, for example, those by (Vilnay 1988, Roberts 1989, Roberts and Haji-Kazemi 1989, Taljsten 1997, Malek *et al.* 1998, Maalej and Bian 2001, Teng *et al.* 2001, 2002, 2009, Tounsi and Benyoucef 2007, Deng *et al.* 2004, Shen 2001, Yang 2007, Benachour *et al.* 2008, Guenaneche 2014, Krour 2014, Zidani 2015, Bensaid *et al.* 2015, 2017, Zidi *et al.* 2017, Belabed 2018).

Based on the solution of Tsai *et al.* (1998), Tounsi (2006) proposed a famous solution by incorporating the effects of interface shear stress on deformation in adherends, which were ignored by Smith and Teng (2001) when they uncoupled a coupled governing equation. Combining the shear deformable bi-beam theory with a linear elastic interface model, Wang (2003) obtained the stress distribution and fracture along the interface. Tounsi *et al.* (2009) and Qiao and Chen (2008) provided an improved solution and a more accurate prediction compared to the above models. Hao *et al.* (2012) presented an improved analytical solution for interfacial stresses that includes various loading conditions simultaneously, including prestress, mechanical and thermal loads, and the effects of adherend shear deformations and curvature mismatches between the beam and the plate. Belakhdar *et al.* (2011) analyzed the effect of tapered-end shape of FRP sheets on stress concentration in strengthened beams, they used the finite difference method to solve problems of beams strengthened with plates have complex geometrical extremities. Edalati and Fereidoon (2012) an analytical method to calculate the interfacial shear and normal stresses in reinforced concrete developed (RC) beams strengthened by a fiber reinforced polymer (FRP) sheet or a steel plate. Touati *et al.* (2015) presented an improved analytical solution to consider the effect of shear deformation on adhesive stresses in plated concrete beams, in their analysis a new originality was presented by considering the shear deformation in the normal stress independently to the shear stress. (Zhou *et al.* 2017, Wu *et al.* 2018) conducted experimental studies on interfacial shear stresses distribution between concrete and FRP sheets. Brairi *et al.* (2018) provided a new analytical solution to predict the interfacial stresses of a functionally graded beam reinforced by a prestressed CFRP plate and subjected to thermo-mechanical loading, the obtained results are checked with the FE analysis results employing the ANSYS software. More recently, a new design for reducing interfacial stresses of reinforced structures with FRP plates, by the concept of taper effect was analyzed by Belabed *et al.* (2018) employing Finite element package. Hebbaz *et al.* (2019) presented an improved numerical analysis of structures reinforced by composite FRP subjected to the hygrothermal and prestressing loads. The taper effect was used as an efficient technique to reduce the stresses concentration. Recently, Guenaneche *et al.* (2019) developed an efficient model based on 2D elasticity theory approach to calculate the interfacial stresses in bonded beam by introducing the shear deformation using the equilibrium equations of the elasticity.

It is clear that none of the previous articles on strengthening of damaged structures have considered the shear slip effect at the interfaces in their analysis. It is reported that the mechanical behavior of the repaired bonded beam is significantly influenced by this parameter. In fact, thermal mechanical loading of affected strengthened beam through the present model is a novel topic, which is not reported yet.

This article introduces an improved theoretical model for predicting adhesive shear and normal

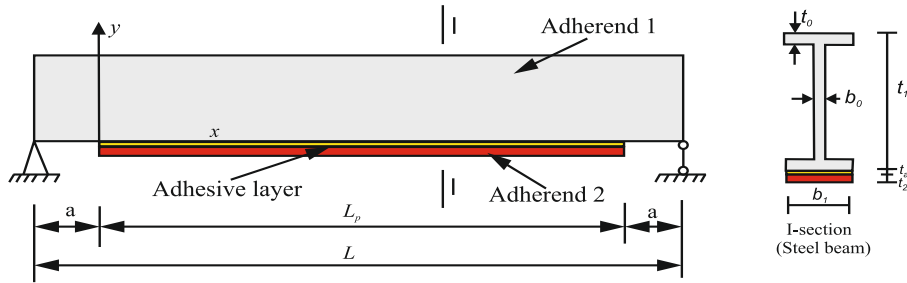


Fig. 1 Steel beam strengthened with bonded thin composite plate. Tounsi (2006)

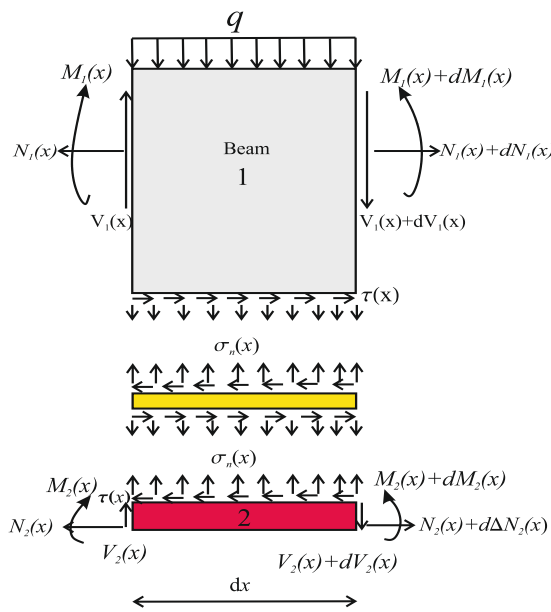


Fig. 2 Infinitesimal element of soffit-plated beam: the loads on the structural element

stresses of externally bonded plate on the steel beam tension surface by including the shear-lag effect of adherends, thermal impact, and mechanical properties of the FRP and adhesive materials for the FRP-strengthened structure. It explicitly considers the interface slip effect on the structural performance. Comparatively to those of the cited methods above, the computed interfacial stresses are considerably smaller than those obtained by other models which neglect adherend shear deformations. Hence, the adopted improved model describes better actual response of FRP–Steel beams and permits the evaluation of interfacial stresses, the knowledge of which is very important in the design of such structures.

2. Mathematical model for bonded repair considering interface slip

Fig. 1 shows the geometrical form of the structure reinforced with its dimensional parameters, thus, that the section according to the section of A-A, represents the configuration of the interface of the adhesive layer. In Fig. 2; the terms V , M , and N denote the shear force, the bending moment,

and the longitudinal tension, respectively, $\tau(x)$ and $\sigma(x)$, denote the shear stress and the normal stress at the interface, respectively, and t represents the component thickness. The subscripts 1 and 2 denote beam and FRP plate, respectively, and show the positive sign convention for the bending moment, shear force, axial force, and applied loading. Four basic assumptions made are: (a) both the two adherends and the adhesive behave in an elastically linear manner; (b) the shear stress in the interface is proportional to the shear slip; (c) the two bonded adherends have the same bending curvature at the same section; (d) since the thickness of the adhesive is small, both the shear and peeling stresses in the adhesive are assumed constant across its thickness.

2.1 Shear stresses along the adhesively bonded interface

The assumption (a) results in

$$\tau(x) = k_{as} S(x), \quad (1)$$

Where $S(x)$ is the shear slip in the interface between the two bonded adherends, $\tau(x)$ is the interfacial shear stress and k_{as} is the shear stiffness of adhesive, which is given by

$$k_{as} = \frac{G_a}{t_a}, \quad (2)$$

Where G_a and t_a are the shear modulus and the thickness of adhesive, respectively.

The real deformed cross-section of each adherend is nonlinear; this deviates from the linear one which was assumed by Tsai *et al.* (1998) and by Tounsi (2006). Recently, Tounsi *et al.* (2009) provided an improved solutions and more accurate predictions compared to the above models. In this respect, it can be expected that the present study should produce results of an even higher accuracy and produce equivalent results to that obtained with high-order theories. Based on this recent work Tounsi *et al.* (2009), the shear-lag effect of the adherends is taken into account in assessing the shear slip $S(x)$ which has been neglected in most existing works, the expression of $S(x)$ is given as

$$S(x) = \left(u_2(x) - \frac{t_2}{2} \left(-\frac{dw_2}{dx} \right) \right) - \left(u_1(x) + \frac{t_1}{2} \left(-\frac{dw_1}{dx} \right) \right) - \left(\frac{t_1}{4G_1} \xi + \frac{5t_2}{12G_2} \right) \tau(x) \quad (3)$$

Where $u_i(x)$ and $w_i(x)$ are the longitudinal middle plane displacements and the vertical displacements of beams (adherends), respectively, and G_i is the shear modulus of adherends i ($i=1, 2$).

A typical infinitesimal isolated body of the plated beam is shown in Fig. 2, and the following equilibrium equations are established

$$\frac{dN_1(x)}{dx} = -b_2 t(x), \quad \frac{dN_2(x)}{dx} = b_2 t(x) \quad (4a)$$

$$\frac{dM_1(x)}{dx} = V_1(x) - b_2 \frac{t_1}{2} \tau(x), \quad \frac{dM_2(x)}{dx} = V_2(x) - b_2 \frac{t_2}{2} \tau(x) \quad (4b)$$

$$\frac{dV_1(x)}{dx} = -r(x) - q, \quad \frac{dV_2(x)}{dx} = r(x) \quad (4c)$$

$$V_1(x) + V_2(x) = V_T(x) \quad (4d)$$

Where $N_1(x)$ and $\Delta N_2(x)$, $V_1(x)$ and $V_2(x)$, $M_1(x)$ and $M_2(x)$ are the internal axial forces, transverse shear forces, and bending moments in adherends 1 and 2, respectively; $V_T(x)$ is the total applied transverse shear force; b_2 is the width of adherend 2 as well as the adhesive layer (see Fig. 1); $\tau(x)$ is the interface shear stress, and $r(x) = b_2\sigma(x)$ is the normal force per unit length between adherend 1 and adherend 2 ($\sigma(x)$ is the normal stress in the interface).

The assumed curvature compatibility between the two bodies gives the curvature ϕ as

$$\phi = \frac{M_1}{E_1 I_1} = \frac{M_2}{E_2 I_2}, \quad (5)$$

Where E_i and I_i are the Young's modulus and the moment of inertia of adherend ($i=1, 2$), respectively.

Solving Eqs. (4)-(5) yields

$$\frac{d\phi}{dx} = \frac{V_T - b_2 d_c \tau(x)}{E_1 I_1 + E_2 I_2}, \quad (6)$$

Where $d_c = (t_1 + t_2)/2$.

According to the Euler-Bernoulli beam theory, the stresses and displacements of individual adherend can be related as

$$N_1(x) = E_1 A_1 \left(\frac{du_1}{dx} - \alpha T_b \right), \quad N_2(x) = E_2 A_2 \frac{du_2(x)}{dx}, \quad M_i(x) = -E_i I_i \frac{d^2 w_i(x)}{dx^2} \quad (7)$$

Where A_i is the cross-sectional area of adherend ' i ' ($i=1, 2$), α , T_b are a linear coefficient of thermal expansion, the temperature distribution. Differentiating Eq. (3) with respect to x once and combining with Eqs. (4), (6) and (7) yield:

$$\frac{dS(x)}{dx} = \frac{N_2(x)}{E_2 A_2} - \frac{N_1(x)}{E_1 A_1} - \alpha T_b - d_c \phi(x) - \left(\frac{t_1}{4G_1} \xi + \frac{5t_2}{12G_2} \right) \frac{d\tau(x)}{dx} \quad (8)$$

Using Eq. (1), the above equation becomes

$$\frac{dS(x)}{dx} = \gamma_s = \frac{K}{K_{as}} \left(\frac{N_2(x)}{E_2 A_2} - \frac{N_1(x)}{E_1 A_1} - \alpha T_b - d_c \phi(x) \right) \quad (9)$$

Where γ_s is the shear slip strain and K is given by

$$K = \frac{1}{\frac{1}{k_{as}} + \frac{t_1}{4G_1} \xi + \frac{5t_2}{12G_2}} \quad (10)$$

Taking a derivative with respect to x in Eq. (14) and then considering Eqs. (4a) and (6), the differential equation of slip displacement S is derived as

$$\frac{d^2 S(x)}{dx^2} = \lambda^2 S(x) - \theta V_T, \quad (11)$$

$$\lambda^2 = Kb_2 \left[\frac{1}{E_1 A_1} + \frac{1}{E_2 A_2} + \frac{d_c^2}{E_1 I_1 + E_2 I_2} \right], \quad (12)$$

$$\theta = \frac{K}{k_{as}} \frac{d_c}{E_1 I_1 + E_2 I_2}. \quad (13)$$

For simplicity, the general solutions presented below are limited to loading which is either concentrated or uniformly distributed over part or the whole span of the beam, or both. For such loading, $d^2 V_T(x)/dx^2 = 0$, and the general solution to Eq. (11) is given by

$$S(x) = B_1 \cosh(\lambda x) + B_2 \sinh(\lambda x) + m_1 V_T(x), \quad (14)$$

$$m_1 = \frac{\theta}{\lambda^2}. \quad (15)$$

The constants B_1 and B_2 are to be determined from boundary conditions defined in the next section 2.1.1

Using Eq. (1), the interfacial shear stress is given by

$$\tau(x) = k_{as} S(x). \quad (16)$$

2.1.1 Application of boundary conditions

By substituting the expression for the shear force in a simply supported beam subjected to a uniformly distributed load into Eq. (14), the general solution for the slip displacement for this load case can be found as

$$S(x) = B_1 \cosh(\lambda x) + B_2 \sinh(\lambda x) + m_1 q \left(\frac{L}{2} - x - a \right), \quad (17)$$

Where q is the uniformly distributed load and x , a , L and L_p are defined in Fig. 1. The constants of integration need to be determined by applying suitable boundary conditions. Considering the boundary conditions:

1. Due to symmetry, the slip displacements at mid-span is zero, i.e.

$$S\left(\frac{L_p}{2}\right) = B_1 \cosh\left(\lambda \frac{L_p}{2}\right) + B_2 \sinh\left(\lambda \frac{L_p}{2}\right) + m_1 V_T\left(\frac{L_p}{2}\right) = 0. \quad (18)$$

2. At the end of the FRP plate, the longitudinal force $[N_1(0)=N_2(0)]$ and the moment $M_2(0)$ are zero. As a result, the moment in the section at the plate curtailment is resisted by the beam alone and can be expressed as

$$M_1(0) = \frac{qa}{2}(L-a). \quad (19)$$

Applying the above boundary condition in Eq. (14)

$$\gamma(x=0) = -m_2 M_1(0), \quad m_2 = \frac{K}{K_{as}} \left(\frac{d_c}{E_1 I_1} + \frac{\alpha T_b}{M_1(0)} \right) \quad (20)$$

From the above three equations

$$B_2 = \frac{-m_2 qa}{2\lambda}(L-a) + \frac{m_1}{\lambda}q, \quad (21)$$

$$B_1 = -B_2 \tanh\left(\frac{\lambda L_p}{2}\right). \quad (22)$$

For practical cases $\lambda L_p/2 > 10$ and as a result $\tanh(\lambda L_p/2) \approx 1$. So the expression for B_1 can be simplified to:

$$B_1 = -B_2 \quad (23)$$

By substituting the expressions of B_1 and B_2 into equation (12) gives an expression for the interfacial shear stress at any point:

$$S(x) = \left(\frac{m_2 a}{2}(L-a) - m_1\right) \frac{qe^{-\lambda x}}{\lambda} + m_1 q \left(\frac{L}{2} - a - x\right), \quad 0 \leq x \leq L_p \quad (24)$$

2.2 Normal stresses along the adhesively bonded Interface

The normal force $r(x)$ in the interface is regarded as a distributed load for adherend 2 and can thus be calculated considering Eqs. (4)-(6) as

$$r(x) = k_{as} b_2 \left[\frac{t_2}{2} - d_c \frac{E_2 I_2}{E_1 I_1 + E_2 I_2} \right] \gamma_s(x). \quad (25)$$

Physically, both the shear force and bending moment at the end of adherend 2 (free end of the bonded plate) should be zero. However, since the shear interface stress τ is not zero at this point, the boundary condition of $V_2=0$ at this point cannot be fulfilled. In addition, for adherend 2 to maintain the same curvature as adherend 1, $M_2=0$ at this free end cannot be satisfied either. To correct this boundary condition, this non-zero values can be calculated and equal and opposite forces can be applied to the ends of FRP plate. The vertical force at the end of FRP plate can be derived by equilibrium

$$V_2(0) = \frac{E_2 I_2}{E_1 I_1 + E_2 I_2} V_T + k_{as} b_2 \left[\frac{t_2}{2} - d_c \frac{E_2 I_2}{E_1 I_1 + E_2 I_2} \right] S(0). \quad (26)$$

From Eq. (9), the non-zero moment of FRP plate at the end of plate is calculated as

$$M_2(0) = \frac{E_2 I_2}{E_1 I_1} M_1(0). \quad (27)$$

The shear force in Eq. (26) and the moment in Eq. (27) are applied back to the ends of FRP plate to correct the incompatible boundary conditions. Assume that the section dimensions of concrete beam are much larger than those of FRP plate (such as in the case of beams repaired with thin plates) and these correction forces are relatively small, the deformation of concrete beam due to these correction forces is then negligible and assumed to be rigid in this calculation.

The calculation model will then be reduced to a beam (FRP plate) on an elastic foundation (adhesive) with a vertical spring stiffness of k_{as} . Using the theory of a beam on an elastic foundation,

Table 1 Geometric and material parameters

Component	Width b (mm)	Depth t (mm)	E (GPa)	ν
Structure	$b_1=250$	$t_1=600$	$E_1=100$	0.28
Adhesive layer	$b_a=240$	$t_a=12$	$E_a= 10$	0.35
Composite plate	$b_2=240$	$t_2=2.0$	$E_2=310$	0.35

we have the vertical displacement of FRP plate as

$$w = \frac{e^{-\chi}}{k_{an}} \left[2\beta_s V_2(0) \cos(\chi) - 2\beta_s^2 M_2(0) (\cos(\chi) - \sin(\chi)) \right], \quad (28)$$

where

$$\chi = \beta_s \cdot x, \quad (29)$$

$$\beta_s = \left(\frac{k_{an}}{4E_2 I_2} \right)^{1/4}, \quad (30)$$

$$k_{as} = \frac{E_a b_2}{G_a}, \quad (31)$$

Where E_a is the elastic modulus of the adhesive.

The total normal stress σ in the interface (from both the external vertical force and the boundary correction forces) is derived as

$$\sigma(x) = \frac{r + k_{an} w}{b_2} \quad (32)$$

3. Results and discussion

In this research, the numerical solution shows that the interfacial stresses are significant at the end of the FRP plate and that their values decrease after a limit of 100 mm. All the solutions used to identify the interfacial stresses converge and according to several approaches analyzed in several works that exist in the literature. The uniformly distributed load is 500 KN/m² and, the coefficient of thermal expansion of the beam has a middle value 10.2 10⁻⁶/°C.

A summary of the geometric and material properties is given in Table 1.

3.1 Comparisons with existing models

3.1.1 Analytical model agreement.

In this section, numerical results of the present solutions are presented to study the effect of various parameters on the distributions of the interfacial stresses in an RC, Aluminium, or Steel beam bonded with an FRP plate. The results are intended to demonstrate the main characteristics of interfacial stress distributions in these strengthened beams. This method is verified by comparing it to the closed-form solution presented by Smith and Teng (2001), Tounsi *et al.* (2009) and by Wang

Table 2 Comparison of the maximum values of interfacial stresses (different configurations)

Theory	Shear stress τ (MPa)	Normal stress σ (MPa)
Smith and Teng (2001)	2.740	1.448
Tounsi <i>et al.</i> (2009)	1.602	0.982
Wang (2003)	2.424	1.955
Present work	Case 1	0.859
	Case 2	0.846
	Case 3	4.412

Note: Present work (Case 1): mechanical load; present work (Case 2): mechanical load with ShearLag ; present work (Case 3): mechanical and thermal load.

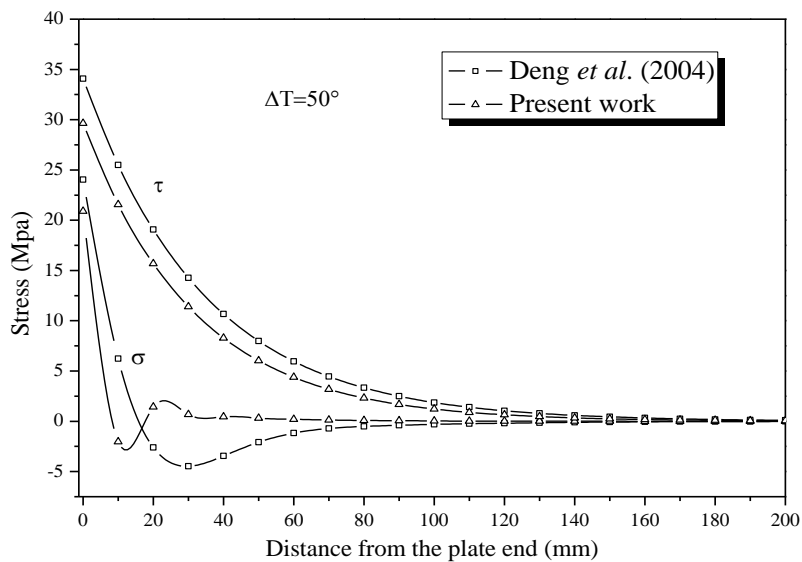


Fig. 3 Comparison of Interfacial stresses: thermal load

et al. (2003), see Table 2. The closed-form solution given by Smith and Teng improves the more accurate widely applicable solution, particularly when the flexural stiffness of the bonded plate becomes significant.

From the presented results presented above, we can see an excellent agreement between these methods. Overall, the predictions of the different solutions agree closely with each other and we noticed that the bending deformation and the axial load are the determining elements in the assembly structures but the thermal shear deformations are the dominant parameters in the retrofit operations of the structures. In this study, thermal loads coupled with mechanical load are the dominant parameters in the retrofit operations of the structures, particularly in design of civil structures and rehabilitation. This originality research is described in terms by the analysis of the stages 1, 2 and 3, and is likely to be the most accurate for the interfacial stresses as given bellow, as plotted in Figs. 3-5.

In Fig. 3, one presents the effect of the thermal distribution of the stresses values. It shows the influence of the temperature, and that can be justified as follows: The thermal effect on the structure and the composite reinforcement can cause possible impact and ruptures of the structure; Smith and

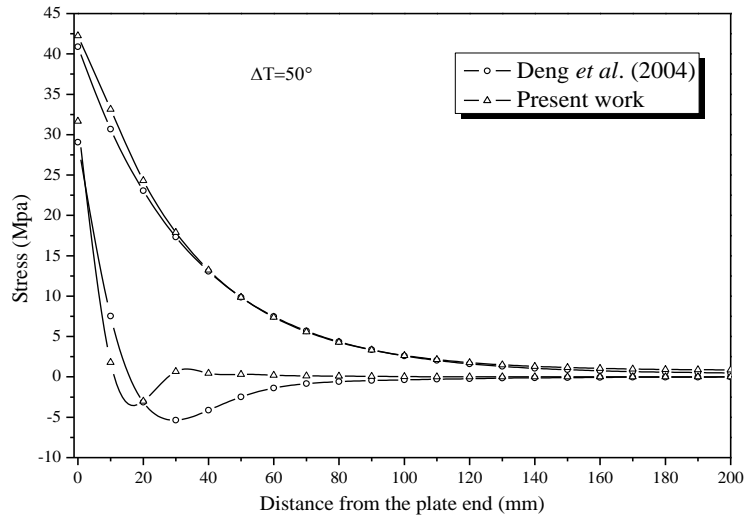


Fig. 4 Interfacial stresses comparison: mechanical and thermal loads

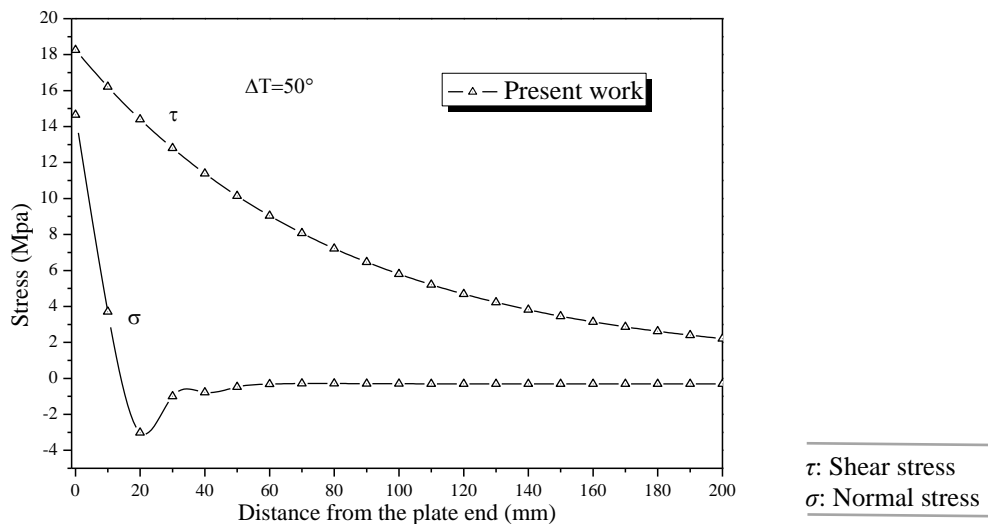


Fig. 5 Interfacial stresses comparison: thermal and mechanical loads with shear lag effect

Teng (2001), Tsai *et al.* (1998).

The results obtained using the method developed by these researches together with the present closed-form solution for interfacial shear and normal stresses are shown in Table 2. As can be seen Fig. 4 illustrates the variation of the interfacial stresses according to the mechanical and thermal load. It makes it possible to see the coupled effect of the two load interfacial stresses and the evolution of the interfacial stresses.

Fig. 5 illustrates the variation of the constraints of interface according to the mechanical and thermal load coupled with shear lag effect. It is the effect of coupling between the three models (mechanical, thermal and shear lag) and their influence on the structure, which was not studied by the preceding studies.

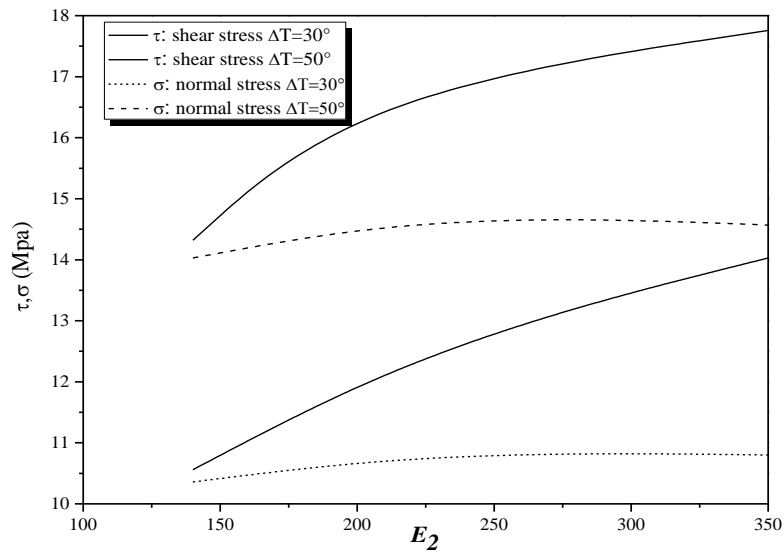


Fig. 6 Interfacial stresses: composite elastic modulus effect (E_2)

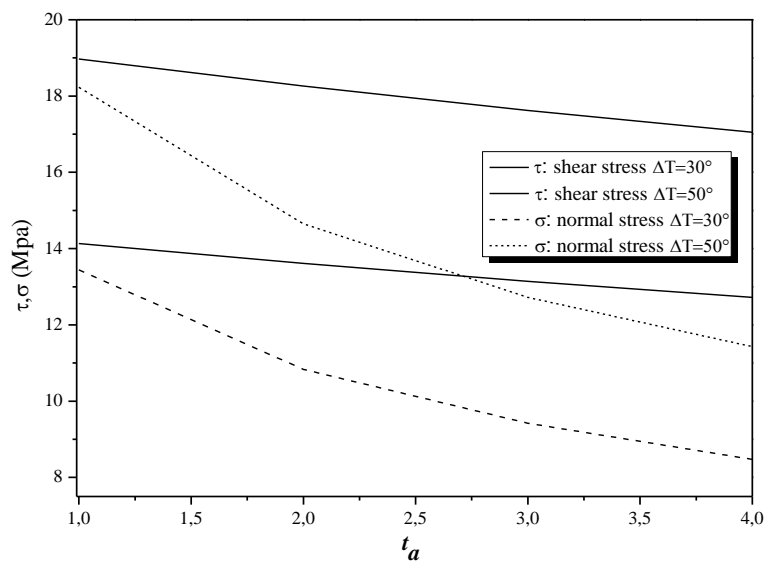


Fig. 7 Effect of adhesive layer thickness on interfacial stresses in FRP strengthened beam

4. Parametric study

4.1 Physical and geometrical parameters influence

One represents the results concerning the physical and geometrical parameters. Fig. 6 illustrates the maximum variation of interfacial stresses with the increase in the elastic modulus of the composite. Fig. 7 illustrates the minimal variation of the stresses with the increase adhesive thickness. Fig. 8 illustrates the maximum variation of the interfacial stresses with the increase

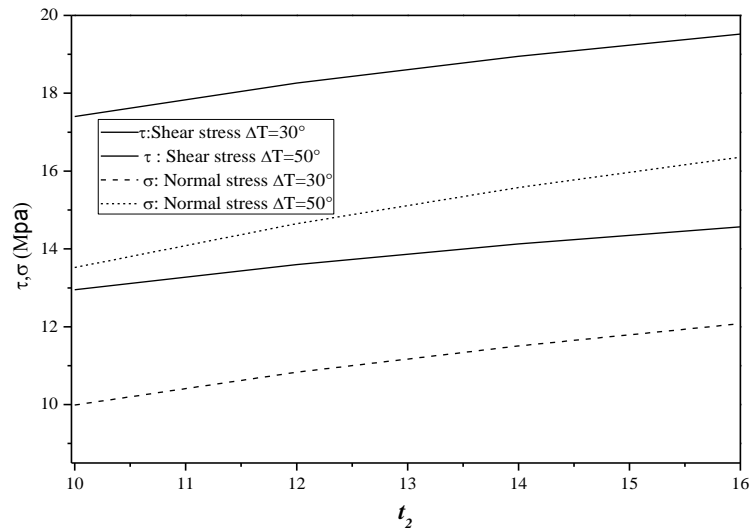


Fig. 8 Interfacial stresses: composite plate thickness (t_2)

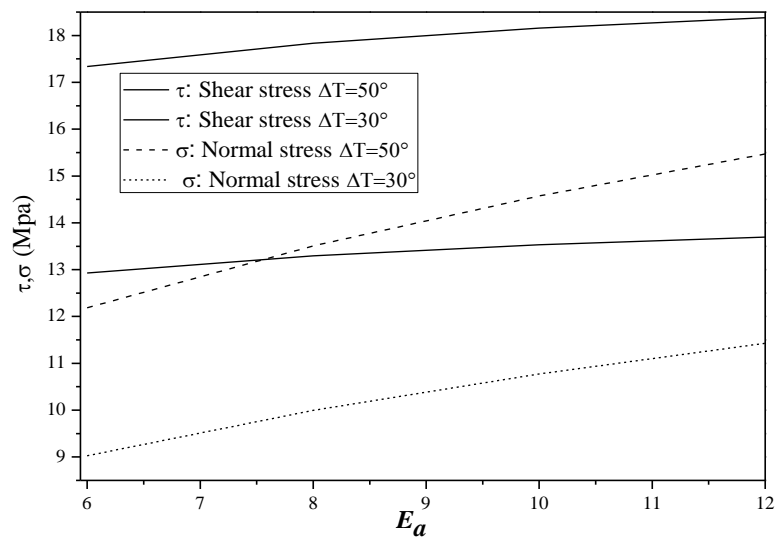


Fig. 9 Effect of adhesive elastic modulus on the stresses value

composite plate thickness. Fig. 9 illustrates the maximum variation of the stresses with the increase in the adhesive elastic modulus.

4.1.1 Effect of FRP strip thickness

Fig. 6 gives interfacial normal and shear stresses for the Steel beam bonded with CFRP plate which demonstrates the effect of plate material properties on interfacial stresses. The results show that, as the plate material became softer, the interfacial stresses become smaller. The peak of interfacial shear and normal stresses moves close to the free edge as the FRP plate, ($\tau_{max}=15.42$ MPa; $\sigma_{max}=7.64$ MPa).

4.1.2 Effect of adhesive layers thickness

Fig. 7 shows the effects of the thickness of the adhesive layer on the interfacial stresses. It is seen that increasing the thickness of the adhesive layer leads to significant reduction in the peak interfacial stresses. The maximum values of adhesive stresses are reached at the plate end region ($\tau_{\max}=16.54$ MPa; $\sigma_{\max}=10.79$ MPa).

4.1.3 Effect of FRP strip thickness

Fig. 8 shows the effects of the thickness of the FRP plate on the interfacial stresses. It is shown that the level and concentration of interfacial stresses are influenced considerably by the thickness of FRP plate. Thus any increase in the FRP thickness leads to an increase in the magnitude of the edge stresses ($\tau_{\max}=11.77$ MPa; $\sigma_{\max}=6.89$ MPa). Therefore, the fact of the smaller interfacial stress level and concentration should be one advantage of retrofitting by FRP over by steel plate.

4.1.4 Effect of the adhesive rigidity

The values of the shear stress and the normal stress at the free edges of the composite plate are shown in Fig. 9. We clearly deduced that the stiffness of the adhesive considerably reduces the values of interfacial stresses. More of rigidity increases more the value of stresses increases, ($\tau_{\max}=8,3$ MPa; $\sigma_{\max}=10,7$ MPa).

5. Conclusions

An improved closed-form solution method is presented in this paper for predicting the interfacial normal and shear stresses of a plated beam under thermal and mechanical loads by considering explicitly the interface slip effect. The previous studies ignored terms, such as the contribution of the adherend shear deformations coupled with thermal effect in the existing solutions, have been included in the present model. The solutions were then modified to satisfy the boundary conditions by applying derived correction forces back to the ends of the repairing plate through a beam-on-elastic-foundation approach. The improved solutions have been validated by comparing them with the existing solutions. All of the existing solutions include the bending and the axial deformations in the structures with omission of other terms, but the new solution includes the effects of all solicitations terms, like the shear deformations of the thermal loads coupled with mechanical load. The interfacial stresses are influenced by the geometry and material parameters, such as, shear modulus and thickness of adhesive layer, elastic modulus and thickness of FRP plate, and the fiber orientation of the different degrees. In future, more extensive work is required to solve the problems caused by the change in temperature, moisture, and fatigue damage of the interface of FRP-strengthened structures.

References

- Belabed, Y., Kerboua, B. and Tarfaoui, M. (2019), "New design for reducing interfacial stresses of reinforced structures with FRP plates", *Int. J. Build. Pathol. Adapt.*, **37**(2), 196-207. <https://doi.org/10.1108/IJBPA-09-2018-0073>.
- Belabed, Z., Bousahla, A.A., Houari, M.S.A., Tounsi, A. and Mahmoud, S.R. (2018), "A new 3-unknown hyperbolic shear deformation theory for vibration of functionally graded sandwich plate", *Earthq. Struct.*,

- 14(2), 103-115. <https://doi.org/10.12989/eas.2018.14.2.103>.
- Belakhdar, K., Tounsi, A., Adda Bedia, E.A. and Yeghnem, R. (2011), "Effect of tapered-end shape of FRP sheets on stress concentration in strengthened beams", *Steel Compos. Struct.*, **11**(6), 435-454. <https://doi.org/10.12989/scs.2011.11.6.435>.
- Benachour, A., Benyoucef, S., Tounsi, A. and Adda Bedia, E.A. (2008), "Interfacial stress analysis of steel beams reinforced with bonded prestressed FRP plate", *Eng. Struct.*, **30**, 3305-3315. <https://doi.org/10.1016/j.engstruct.2008.05.007>.
- Bensaid, I. and Kerboua, B. (2017), "Interfacial stress analysis of functionally graded beams strengthened with a bonded hygrothermal aged composite plate", *Compos. Interf.*, **24**(2), 149-169. <https://doi.org/10.1080/09276440.2016.1196333>.
- Bensaid, I., Kerboua, B. and Cheikh, A. (2015), "Interfacial stresses analysis of damaged structures strengthened with bonded prestressed FRP plate having variable fiber spacing", *Int. J. Struct. Integr.*, **6**(2), 159-175. <https://doi.org/10.1108/IJSI-02-2014-0006>.
- Brairi, S., Kerboua, B. and Bensaid, I. (2018), "Improved stresses analysis of a functionally graded beam under prestressed CFRP plate", *Adv. Compos. Lett.*, **27**(1), 10-22. <https://doi.org/10.1177/096369351802700102>.
- Cai, C.S., Nie, J. and Shi, X.M. (2007), "Interface slip effect on bonded plate repairs of concrete beams", *Eng. Struct.*, **29**, 1084-1095. <https://doi.org/10.1016/j.engstruct.2006.07.017>.
- Chikh, A., Tounsi, A., Hebali, H. and Mahmoud, S.R. (2017), "Thermal buckling analysis of cross-ply laminated plates using a simplified HSDT", *Smart Struct. Syst.*, **19**(3), 289-297. <https://doi.org/10.12989/sss.2017.19.3.289>.
- Deng, J., Lee, M.M.K. and Moy, S.S.J. (2004), "Stress analysis of steel beams reinforced with a bonded CFRP plate", *Compos. Struct.*, **65**, 205-215. <https://doi.org/10.1016/j.compstruct.2003.10.017>.
- Draiche, K., Benyoucef, S., Tounsi, A. and Adda Bedia, E.A. (2019), "Improved analytical method for adhesive stresses in plated beam: Effect of shear deformation", *Adv. Concrete Constr.*, **7**(3), 151-166. <https://doi.org/10.12989/acc.2019.7.3.151>.
- Edalati, M. and Irani, F. (2012), "Interfacial stresses in RC beams strengthened by externally bonded FRP/steel plates with effects of shear deformations", *J. Compos. Constr.*, **16**(1), 60-73. [https://doi.org/10.1061/\(ASCE\)CC.1943-5614.0000238](https://doi.org/10.1061/(ASCE)CC.1943-5614.0000238).
- Guenaneche, B., Benyoucef, S., Tounsi, A. and Adda Bedia, E.A. (2019), "Improved analytical method for adhesive stresses in plated beam: Effect of shear deformation", *Adv. Concrete Constr.*, **7**(3), 151-166. <https://doi.org/10.12989/acc.2019.7.3.151>.
- Guenaneche, B., Tounsi, A. and Adda Bedia, E.A. (2014), "Effect of shear deformation on interfacial stress analysis in plated beams under arbitrary loading", *Adhes. Adhesiv.*, **48**, 1-13. <https://doi.org/10.1016/j.ijadhadh.2013.09.016>.
- Hao, S.W., Liu, Y. and Liu, X.D. (2012), "Improved interfacial stress analysis of a plated beam", *Struct. Eng. Mech.*, **44**(6), 815-837. <https://doi.org/10.12989/sem.2012.44.6.815>.
- Hebbaz, M.A., Kerboua, B. and Tarfaoui, M. (2019), "Improved numerical analysis of structures reinforced by composite FRP: Hygrothermal and prestressing loads with taper effect", *Adv. Compos. Lett.*, **28**, 1-9. <https://doi.org/10.1177/0963693519858364>.
- Kerboua, B., Bensaid, I. and Adda Bedia, E. (2013), "Impact of interfacial stresses distribution of structures reinforced by composites FRP: new model of the laminate layers", *J. Adhe. Sci. Tech.*, **27**(17), 1853-1865. <https://doi.org/10.1080/01694243.2012.763020>.
- Krou, B., Bernard, F. and Tounsi, A. (2014), "Fibers orientation optimization for concrete beam strengthened with a CFRP bonded plate: A coupled analytical-numerical investigation", *Eng. Struct.*, **56**, 218-227. <https://doi.org/10.1016/j.engstruct.2013.05.008>.
- Maalej, M. and Bian, Y. (2001), "Interfacial shear stress concentration in FRP-strengthened beams", *Compos. Struct.*, **54**, 417-426. <https://doi.org/10.1016/j.engstruct.2013.05.008>.
- Malek, A.M., Saadatmanesh, H. and Ehsani, M.R. (1998), "Prediction of failure load of R/C beams strengthened with FRP plate due to stress concentration at the plate end", *ACI Struct. J.*, **95**(1), 142-152.
- Merdaci, S., Tounsi, A. and Bakora, A. (2016), "A novel four variable refined plate theory for laminated

- composite plates”, *Steel Compos. Struct.*, **22**(4), 713-732. <https://doi.org/10.12989/scs.2016.22.4.713>.
- Qiao, P. and Chen, F. (2008), “An improved adhesively bonded bi-material beam model for plated beams”, *Eng. Struct.*, **30**(7), 1949-57. <https://doi.org/10.1016/j.engstruct.2007.12.017>.
- Roberts, T.M. (1989), “Approximate analysis of shear and normal stress concentrations in the adhesive layer of plated RC beams”, *Struct. Eng.*, **67**(12), 229-233.
- Roberts, T.M. and Haji-Kazemi, H. (1989), “Theoretical study of the behavior of reinforced concrete beams strengthened by externally bonded steel plates”, *Proc. Inst. Civil Eng.*, **87**, 39-55. <https://doi.org/10.1680/iicep.1989.1452>.
- Smith, S.T. and Teng, J.G. (2001), “Interfacial stresses in plated RC beams”, *Eng. Struct.*, **23**(7), 857-871. [https://doi.org/10.1016/S0141-0296\(00\)00090-0](https://doi.org/10.1016/S0141-0296(00)00090-0).
- Täljsten, B. (1997), “Strengthening of beams by plate bonding”, *J. Mater. Civil Eng.*, ASCE, **9**(4), 206-212. [https://doi.org/10.1061/\(ASCE\)0899-1561\(1997\)9:4\(206\)](https://doi.org/10.1061/(ASCE)0899-1561(1997)9:4(206)).
- Teng, J.G., Zhang, J.W. and Smith, S.T. (2002) “Interfacial stresses in reinforced concrete beams bonded with a soffit plate: A finite element study”, *Constr. Build. Mater.*, **16**, 1-14. [https://doi.org/10.1016/S0950-0618\(01\)00029-0](https://doi.org/10.1016/S0950-0618(01)00029-0).
- Touati, M., Tounsi, A. and Benguediab, M. (2015), “Effect of shear deformation on adhesive stresses in plated concrete beams: Analytical solutions”, *Comput. Concrete*, **15**(3), 141-166. <https://doi.org/10.12989/cac.2015.15.3.337>.
- Tounsi, A. (2006), “Improved theoretical solution for interfacial stresses in concrete beams strengthened with FRP plate”, *Int. J. Solid. Struct.*, **43**, 4154-4174. <https://doi.org/10.1016/j.ijsolstr.2005.03.074>.
- Tounsi, A. and Benyoucef, S. (2007), “Interfacial stresses in externally FRP-plated concrete beams”, *Int. J. Adhes. Adhes.*, **27**, 207-215. <https://doi.org/10.1016/j.ijadhadh.2006.01.009>.
- Tounsi, A., Hassaine Daouadji, T., Benyoucef, S. and Addabedia, E.A. (2009), “Interfacial stresses in FRP-plated RC beams: Effect of adherend shear deformations”, *Int. J. Adhes. Adhes.*, **29**, 343-351. <https://doi.org/10.1016/j.ijadhadh.2008.06.008>.
- Tsai, M.Y., Oplinger, D.W. and Morton, J. (1998), “Improved theoretical solutions for adhesive lap joints”, *Int. J. Solid. Struct.*, **35**(12), 1163-1185. [https://doi.org/10.1016/S0020-7683\(97\)00097-8](https://doi.org/10.1016/S0020-7683(97)00097-8).
- Vilnay, O. (1988), “The analysis of reinforced concrete beams strengthened by epoxy bonded steel plates”, *Int. J. Cement Compos. Lightw. Concrete.*, **10**, 73-78. [https://doi.org/10.1016/0262-5075\(88\)90033-4](https://doi.org/10.1016/0262-5075(88)90033-4).
- Wang, J.L. (2003), “Mechanics and fracture of hybrid material interface bond”, Ph.D. Dissertation, Department of Civil Engineering, The University of Akron, Akron, OH, USA.
- Wu, Q., Xiao, S. and Iwashita, K. (2018), “Experimental study on the interfacial shear stress of RC beams strengthened with prestressed BFRP rod”, *Result. Phys.*, **10**, 427-433. <https://doi.org/10.1016/j.rinp.2018.06.007>.
- Yang, J., Chen, J.F. and Teng, J.G. (2009), “Interfacial stress analysis of plated beams under symmetric mechanical and thermal loading”, *Constr. Build. Mater.*, **23**, 2973-2987. <https://doi.org/10.1016/j.conbuildmat.2009.05.004>.
- Zhou, A., Qin, R., Feo, L., Penna, R. and Lau, D. (2017), “Investigation on interfacial defect criticality of FRP-bonded concrete beams”, *Compos. Part B: Eng.*, **113**, 80-90. <https://doi.org/10.1016/j.compositesb.2016.12.055>.
- Zidani, M.B., Belakhdar, K., Tounsi, A. and Adda Bedia, E.A. (2015), “Finite element analysis of initially damaged beams repaired with FRP plates”, *Compos. Struct.*, **134**, 429-439. <https://doi.org/10.1016/j.compstruct.2015.07.124>.
- Zidi, M., Houari, M.S.A., Tounsi, A., Bessaim, A. and Mahmoud, S.R. (2017), “A novel simple two-unknown hyperbolic shear deformation theory for functionally graded beams”, *Struct. Eng. Mech.*, **64**(2), 145-153. <https://doi.org/10.12989/sem.2017.64.2.145>.